Efficiencies of photoinduced electron-transfer reactions: Role of the Marcus inverted region in return electron transfer within geminate radical-ion pairs

ARTICLE *in* JOURNAL OF THE AMERICAN CHEMICAL SOCIETY · MAY 1990

Impact Factor: 12.11 · DOI: 10.1021/ja00167a027

4 AUTHORS, INCLUDING:

Jacques-E. Moser
École Polytechnique Fédérale de Lausanne
170 PUBLICATIONS **16,052** CITATIONS

coupling obtained in our quasi-one-dimensional approach, but since no experimental value is available, we have not pursued this point. Of course the calculation would be much more difficult for a coupling strong enough to change the level splittings by amounts comparable to the level spacings.

Table IX summarizes the results obtained thus far by ourselves and others on the inversion of free radicals in which the radical center is part of a small ring with or without heteroatoms. The rate constants listed for 353 and 0 K are calculated ("extrapolated") from the available experimental data by means of a quasi-one-dimensional procedure based on the calculation of level splittings. This method is found to be reliable for the systems studied. We therefore conclude that the method of vibronic level splittings, when properly adjusted for contributions of additional degrees of freedom, is satisfactory for tunneling rates in the range measurable by EPR techniques.

Efficiencies of Photoinduced Electron-Transfer Reactions: Role of the Marcus Inverted Region in Return Electron Transfer within Geminate Radical-Ion Pairs

Ian R. Gould,* Deniz Ege, Jacques E. Moser,† and Samir Farid*

Contribution from the Eastman Kodak Company, Corporate Research Laboratories, Rochester, New York 14650-2109. *Received November 24, 1989*

Abstract: In photoinduced electron-transfer processes the primary step is conversion of the electronic energy of an excited state into chemical energy retained in the form of a redox (geminate radical-ion) pair ($A + D \xrightarrow{h\nu} A^{\bullet-}/D^{\bullet+}$). In polar solvents, separation of the geminate pair occurs with formation of free radical ions in solution. The quantum yields of product formation, from reactions of either the free ions, or of the geminate pair, are often low, however, due to the return electron transfer reaction ($A^{\bullet-}/D^{\bullet+} \rightarrow A + D$), an energy-wasting step that competes with the useful reactions of the ion pair. The present study was undertaken to investigate the parameters controlling the rates of these return electron transfer reactions. Quantum yields of free radical ion formation were measured for ion pairs formed upon electron-transfer quenching of the first excited singlet states of cyanoanthracenes by simple aromatic hydrocarbon donors in aceonitrile at room temperature. The free-ion yields are determined by the competition between the rates of separation and return electron transfer. By assuming a constant rate of separation, the rates of the return electron transfer process are obtained. These highly exothermic return electron transfer reactions ($-\Delta G_{-et} = 2-3$ eV) were found to be strongly dependent on the reaction exothermicity. The electron-transfer rates showed a marked *decrease* (ca. 2 orders of magnitude in this ΔG_{-et} range) with *increasing* exothermicity. This effect represents a clear example of the Marcus "inverted region". Semiquantum mechanical electron-transfer theories were used to analyze the data quantitatively. The electron-transfer rates were found also to depend upon the degree of charge delocalization within the ions of the pair, which is attributed to variations in the solvent reorganization energy and electronic coupling matrix element. Accordingly, mostly on the basis of redox potentials, one can vary the quantum yield of free-ion formation from a few percent to values approaching unity. Use of a strong donor with a strong acceptor to induce reactions based on electron transfer is likely to be inefficient because of the fast return electron transfer in the resulting low-energy ion pair. A system with the smallest possible driving force for the initial charge-separation reaction results in a high-energy, and therefore long-lived ion pair, which allows the desired processes to occur more efficiently. The use of an indirect path based on secondary electron transfer, a concept called "cosensitization", results in efficient radical-ion formation even when the direct path results in a very low quantum yield.

I. Introduction

Many examples of photoinduced electron-transfer reactions of organic molecules have been identified.[1] For efficient reaction, the excited-state energy of the species that absorbs the light, either the donor or the acceptor, should be higher than the energy required to reduce the acceptor to its radical anion and oxidize the donor to its radical cation. This situation is illustrated in Scheme I for the case of a singlet excited acceptor A in the presence of a donor D. For such reactions it is well-known that second-order electron-transfer quenching of the excited state by the redox partner occurs efficiently to form primary charge-separated species such as exciplexes and solvated geminate radical-ion pairs (k_{et}, Scheme I).[2] Very often these reactions are performed in polar solvents (usually acetonitrile) to facilitate the solvation of the primary geminate radical-ion pairs into free radical ions in solution (k_{sep}, Scheme I). The chemical products of reactions under these conditions are typical of those expected for free radical ions.[1] The maximum quantum yield for such reactions, in the absence of chain amplification or chemical reaction within the geminate radical-ion pairs, is thus given by the quantum yield

Scheme I. Energy Diagram for Photoinduced Electron Transfer

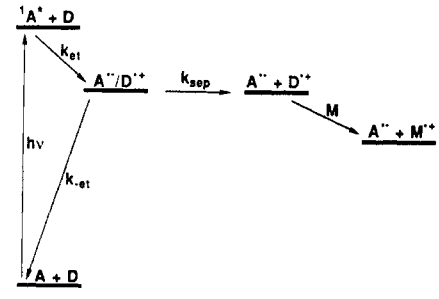

for formation of the free radical ions via solvation and separation processes.[1a,3] However, solvation and separation of the radical

†Current address: Institut de Chimie Physique, Ecole Polytechnique Fédérale, CH-1015 Lausanne, Switzerland.

(1) (a) Mattes, S. L.; Farid, S. In *Organic Photochemistry*; Padwa, A., Ed.; Marcel Dekker: New York, 1983; Vol. 6, p 233. (b) Davidson, R. S. In *Advances in Physical Organic Chemistry*; Gold, V., Bethell, D., Eds.; Academic Press: London, 1983; Vol. 19, p 130. (c) Mattes, S. L.; Farid, S. *Science* **1984**, *226*, 917. (d) Kavarnos, G. J.; Turro, N. J. *Chem. Rev.* **1986**, *86*, 401. (e) *Photoinduced Electron Transfer, Part C. Photoinduced Electron Transfer Reactions: Organic Substrates*; Fox, M. A., Chanon, M., Eds.; Elsevier: Amsterdam, 1988. (f) Mattay, J. *Synthesis* **1989**, 233.

0002-7863/90/1512-4290$02.50/0

Chart I. Alkylbenzene Donors in Order of Decreasing Oxidation Potential

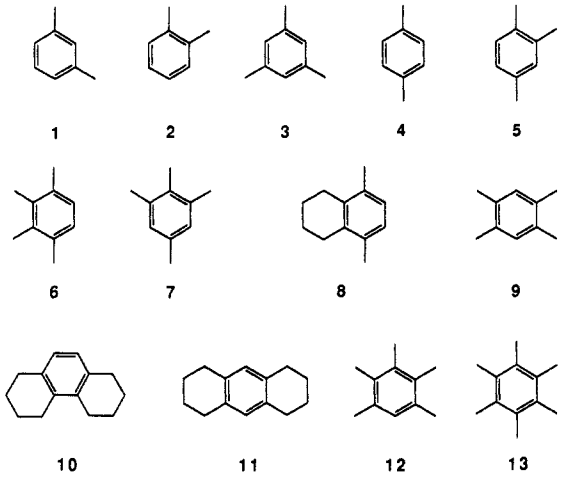

ions always have to compete with the first-order return electron transfer in the geminate pair to re-form the starting materials (k_{-et}, Scheme I).[1a,3,4] Usually this return electron transfer is very efficient and thus the quantum yields for free radical ion formation are usually rather low.[1,3,4]

Careful analysis of the quantum yields for formation of products in the photoinduced electron-transfer reactions of cyanoanthracenes with olefins and acetylenes in acetonitrile suggested that a relationship exists between the rate of the return electron transfer process and the energy content of the radical-ion pair.[1a,c,4] In general, more efficient separation into free ions was observed when the energy content of the ion pair was high. The exothermicity of the return electron transfer reaction is greatest for the ion pairs with the highest energy content, and so the data suggested that an inverse relationship existed between the rate of the reaction and the exothermicity, with those reactions having the highest exothermicity being the slowest.[1a,c,4]

With this information we designed an experiment specifically to test the relationship between the kinetics and the thermodynamics of the return electron transfer reaction. The ion pairs we have studied are those formed upon diffusion-controlled electron-transfer quenching of the first excited states of cyanoanthracenes by simple aromatic hydrocarbon donors in acetonitrile at room temperature. The free radical ions that escape the geminate radical-ion pair are observed directly by transient absorption spectroscopy. Systems were chosen so that chemical reactions within the geminate pair were not important. The results of these experiments clearly define the factors that control the rates of return electron transfer in the geminate radical-ion pairs.

Most of the early studies of electron-transfer processes were concerned with second-order bimolecular reactions in homogeneous solution. However, diffusion effects complicate the analysis of kinetic data under these circumstances. More recently, the importance of studying intramolecular (unimolecular) reactions has been stressed, and in such systems considerable advances have been made in relating electron-transfer experiment with theory (vide infra), although in general, extensions to bimolecular systems have not been emphasized. The return electron transfer reaction in the geminate radical-ion pairs is a bimolecular, first-order reaction in which diffusion effects are not important. Consequently, the radical-ion pairs have proven to be convenient model systems for the study of many aspects of bimolecular electron-transfer reactions.[5]

(2) (a) Beens, H.; Weller, A. In *Organic Molecular Photophysics*; Birks, J. B., Ed.; Wiley: London, 1975; Vol. 2, Chapter 4. (b) Mataga, N. *Pure Appl. Chem.* **1984**, *56*, 1255.

(3) Fox, M. A. In *Advances in Photochemistry*; Volman, D. H., Hammond, G. S., Gollnick, K., Eds.; Wiley: New York, 1986; Vol. 13, p 237.

(4) (a) Mattes, S. L.; Farid, S. *J. Chem. Soc., Chem. Commun.* **1980**, 126. (b) Mattes, S. L.; Farid, S. *J. Am. Chem. Soc.* **1983**, *105*, 1386. (c) Mattes, S. L.; Farid, S. *J. Am. Chem. Soc.* **1986**, *108*, 7356.

Table I. Spectroscopic Properties and Reduction Potentials of the Cyanoanthracene Acceptors in Acetonitrile

acceptor	λ_{max},[a] nm	ϵ_{max}	$E_{0,0}(^1A^*)$,[b] eV	Φ_{fl}	$\tau_{^1A^*}$, ns	$E^{o\prime}$, V (vs SCE)
DCA	422	11,500	2.90	0.88	14.9	−0.91
TCA	428	11,000	2.87	0.92	16.6	−0.44

[a] Maximum of the zero–zero transition of the absorption spectrum. [b] Average energy of the zero–zero transitions of the absorption and emission spectra.

Chart II. Naphthalene and Biphenyl Donors in Order of Decreasing Oxdiation Potential

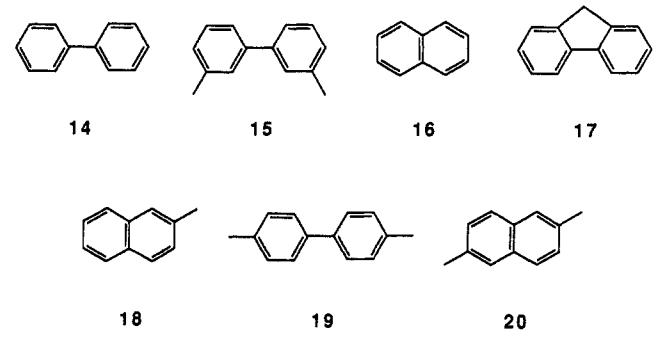

Chart III. Phenanthrene Donors in Order of Decreasing Oxidation Potential

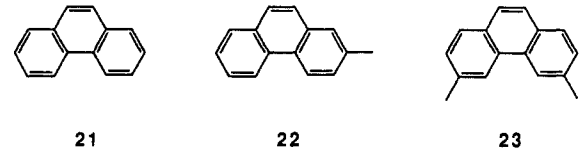

II. Experimental Strategy

The excited-state acceptors used in this work are 9,10-dicyanoanthracene (DCA) and 2,6,9,10-tetracyanoanthracene (TCA) (Table I). The donors are the simple aromatic hydrocarbons shown in Charts I–III. In Chart I are shown alkyl-substituted benzene donors that have only one aromatic ring ("one-ring" donors). In this series of compounds the oxidation potentials are varied over a range of 0.55 V by varying the extent of alkyl substitution on the aromatic ring (vide infra). Substituents with significant steric bulk or heteroatom substituents are deliberately avoided. Shown in Charts II and III are "two-ring" and "three-ring" donors in which the oxidation potentials are varied in the same manner. Within each set of donors, the structural differences are as small as can reasonably be expected while still allowing access to a useful range of oxidation potentials. The mechanism for the quenching of the excited states of the anthracene acceptors (A) by the donors (D) is given in Scheme I. Although Scheme I is clearly oversimplified, it contains all of the important processes necessary to describe the electron-transfer reactions described here. We have previously shown that, for the one-ring donors, chemical reactions do not occur within the geminate radical-ion pair.[5b] According to the mechanism of Scheme I the quantum yield for formation of free radical ions (Φ_{sep}), corrected for incomplete interception of the excited acceptor by the donors, depends upon the rates of ion-pair separation (k_{sep})

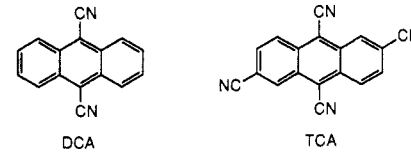

(5) Preliminary accounts of this work have been published: (a) Gould, I. R.; Ege, D.; Mattes, S. L.; Farid, S. *J. Am. Chem. Soc.* **1987**, *109*, 3794. (b) Gould, I. R.; Moser, J. E.; Ege, D.; Farid, S. *J. Am. Chem. Soc.* **1988**, *110*, 1991. (c) Gould, I. R.; Moser, J. E.; Armitage, B.; Farid, S.; Goodman, J. L.; Herman, M. S. *J. Am. Chem. Soc.* **1989**, *111*, 1917.

and return electron transfer (k_{-et}) within the geminate radical-ion pair ($A^{\bullet-}/D^{\bullet+}$), and is given by eq 1. Thus, for a series of ion

$$\Phi_{sep} = \frac{k_{sep}}{k_{sep} + k_{-et}} \quad (1)$$

pairs with differing energy content, the steady-state work[1a,c,4] suggests that different values of Φ_{sep} should be observed, mainly due to changes in k_{-et} for the different radical-ion pairs. The free solvated radical ions that separate from the geminate pair ($A^{\bullet-}$ + $D^{\bullet+}$, Scheme I) can in principle be detected by conventional laser transient absorption spectroscopy and the quantum yields for free radical ion formation obtained directly by using a suitable transient absorption actinometer. However, this approach would require a knowledge of the extinction coefficient and absorption spectrum of each radical ion that is formed. This problem can be avoided by the use of a low concentration of a secondary donor that is lower in oxidation potential than any of the primary donors. In this manner secondary electron transfer will occur from the secondary donor (M, Scheme I) to the primary donor radical cation ($D^{\bullet+}$) with formation of the secondary donor radical cation ($M^{\bullet+}$). In this manner M acts as a monitor for $D^{\bullet+}$, the free radical cations that escape the geminate radical-ion pair. The concentration of the secondary donor (monitor, M) in such experiments should be high enough to react with all of the free radical cations that escape the pair, but low enough so that it does not compete significantly with the primary donor for the cyanoanthracene excited state or intercept the radical-ion pair. In this work we have used 4,4'-dimethoxystilbene, (DMS) tritolylamine (TTA) and trianisylamine (TAA) as free radical cation monitors. The oxidation potentials of these compounds are lower than any of the primary donors by more than 0.4 eV (see Experimental Section), and thus, the secondary electron transfer from M to $D^{\bullet+}$ is diffusion controlled, and reverse electron transfer from D to $M^{\bullet+}$ is not important. The monitor radical cations have absorption maxima in accessible regions of the visible spectra that are characterized by large extinction coefficients. Thus, small concentrations of $M^{\bullet+}$ are easy to detect in transient absorption experiments, and low quantum yields of free ions can be detected by low laser powers. Thus, the relative quantum yields for free-ion formation from a series of ion pairs in the presence of, for example, DMS as a monitor can be determined by measuring the relative optical absorbance of the $DMS^{\bullet+}$ formed by secondary electron transfer. After the free radical cations are scavenged by the DMS, the same transient species are present in solution for all the donor/acceptor pairs, i.e., $DMS^{\bullet+}$ and $DCA^{\bullet-}$ or $TCA^{\bullet-}$ (Scheme I), and thus, the optical absorbances are directly comparable. This comparison is valid for both DCA and TCA since the radical anions of each of these species have similar and much smaller absorbances at the wavelength of observation of the $DMS^{\bullet+}$.[6]

III. Results

A. Transient Absorption Spectroscopy. Pulsed laser excitation at 410 nm of DCA (ca. 5×10^{-5} M) in the presence of 0.2 M biphenyl leads to quenching of the DCA fluorescence (Φ_0/Φ = 10.0 by emission spectroscopy) and the production of a transient absorption spectrum (Figure 1a) due to biphenyl radical cations and DCA radical anions. The absorption spectrum shown is obtained ca. 200 ns after the pulse, before significant second-order diffusional encounter of the free radical cations and anions has occurred. A similar experiment performed in the presence of benzyltrimethylsilane, which scavenges the biphenyl radical cation,[7] resulted in the transient spectrum shown in Figure 1b. The species that is observed under these conditions is susceptible to quenching by dissolved oxygen and is assigned to the DCA radical anion.[8a] Similarly, an experiment performed in the absence of the silane, but in oxygen-purged solution, results in the spectrum shown in Figure 1c. This species has an absorption maximum at 670 nm, which is consistent with that observed upon radiolysis

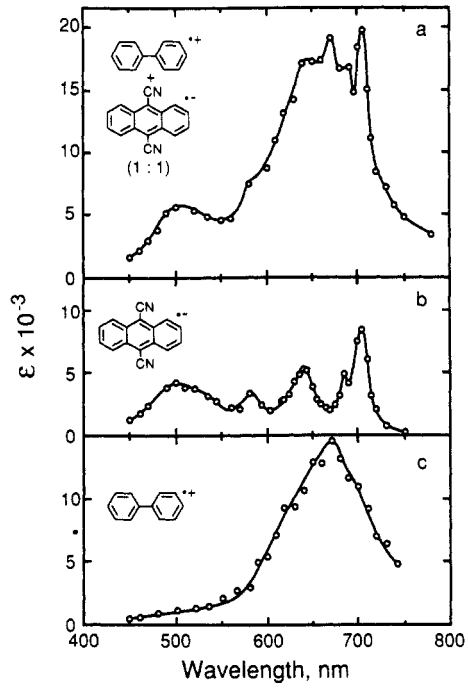

Figure 1. Transient absorption spectra observed upon pulsed laser excitation of 9,10-dicyanoanthracene in the presence of 0.2 M biphenyl in acetonitrile. (a) In the absence of other additives the spectrum is that of a 1:1 mixture of the dicyanoanthracene radical anion and the biphenyl radical cation. (b) Spectrum of the dicyanoanthracene radical anion obtained in the presence of the radical-cation quencher benzyltrimethylsilane. (c) Spectrum of the biphenyl radical cation obtained in the presence oxygen as a DCA radical-anion scavenger.

of biphenyl in low-temperature glasses and assigned to the biphenyl radical cation.[8] Transient absorption spectra have also been obtained for excitation of DCA in the presence of other donors including diphenylacetylene and naphthalene. In each case transient absorptions typical of those expected for the appropriate radical cations are observed.[8,9]

Pulsed laser excitation of a solution of DCA in the presence of biphenyl (0.2 M) and DMS (5×10^{-4} M) results in decay in absorption observed at 670 nm (the maximum of the biphenyl radical cation) and concomitant growth in absorption at 530 nm with a time constant of ca. 200 ns. This observation is consistent with diffusion-controlled quenching of the $biphenyl^{\bullet+}$ by DMS to form the $DMS^{\bullet+}$, which absorbs at 530 nm (Figure 2a). Similar results are obtained with both TTA and TAA as monitors, in which case absorption growth at 670 and 715 nm is observed (Figure 2b and c). In these experiments, the concentrations of the monitor radical cations are equal to those of the initially formed biphenyl radical cation and DCA radical anion. Thus, by use of a value for the extinction coefficient of the $TTA^{\bullet+}$ of 26 200 at 668 nm,[10] extinction coefficients for the $biphenyl^{\bullet+}$ at 670 nm and $DCA^{\bullet-}$ at 705 nm of 14 500 and 7700 are obtained by measuring signal sizes in the presence and absence of the TTA (Figure 1). Similarly, identical concentrations of the monitor radical cations are formed in the secondary electron-transfer reactions, and thus from the ratio of the transient optical densities at their wavelengths

(6) Lenhard, J.; Gould, I. R.; Farid, S., unpublished results.
(7) Dinnocenzo, J. P.; Farid, S.; Goodman, J. L.; Gould, I. R.; Todd, W. P.; Mattes, S. L. *J. Am. Chem. Soc.* **1989**, *111*, 8973.

(8) (a) Shida, T. *Electronic Absorption Spectra of Radical Ions* (*Physical Sciences Data 34*); Elsevier: Amsterdam, 1988. (b) Hamill, W. H. In *Radical Ions*; Kaiser, E. T., Kevan, L., Eds.; Wiley: New York, 1968; Chapter 9.
(9) Gschwind, R.; Haselbach, H. *Helv. Chem. Acta* **1979**, *62*, 941.
(10) The extinction coefficient of the tritolylamine radical cation in acetonitrile was obtained by using quantitative electrochemical oxidation of tritolylamine. We thank J. Lenhard (Eastman Kodak Company) for performing the electrochemical measurement. The extinction coefficients of both the tritolylamine and trianisylamine radical cations were also measured by quantitative chemical oxidation of the neutral amines in acetonitrile using antimony pentachloride. Similar absorption spectra of the radical cations are obtained by the electrochemical, chemical oxidation, and transient absorption techniques, and the extinction coefficients obtained with the three techniques agree within 10%.

Table II. Quantum Yields for Free Radical Ion Formation and Rate Constants for Return Electron Transfer For Radical-Ion Pairs of Cyanoanthracene Radical Anions and Substituted-Benzene "One-Ring" Radical Cations

radical cation	E^{ox}_D,[a] V (vs SCE)	radical anion	$-\Delta G_{-et}$,[b] eV	Φ_{sep}	k_{-et}, s^{-1}
1,2,4-trimethylbenzene (**5**)	1.92	DCA	2.83	0.392	7.76×10^8
1,2,3,4-tetramethylbenzene (**6**)	1.84	DCA	2.75	0.280	1.29×10^9
1,2,3,5-tetramethylbenzene (**7**)	1.83	DCA	2.74	0.274	1.32×10^9
5,8-dimethyltetrahydronaphthalene (**8**)	1.81	DCA	2.72	0.248	1.52×10^9
durene (**9**)	1.78	DCA	2.69	0.239	1.59×10^9
octahydrophenanthrene (**10**)	1.77	DCA	2.68	0.209	1.89×10^9
octahydroanthracene (**11**)	1.72	DCA	2.63	0.203	1.96×10^9
pentamethylbenzene (**12**)	1.71	DCA	2.62	0.154	2.75×10^9
m-xylene (**1**)	2.14	TCA	2.58	0.126	3.47×10^9
o-xylene (**2**)	2.13	TCA	2.57	0.122	3.60×10^9
mesitylene (**3**)	2.11	TCA	2.55	0.093	4.88×10^9
hexamethylbenzene (**13**)	1.59	DCA	2.50	0.078	5.91×10^9
p-xylene (**4**)	2.06	TCA	2.50	0.077	5.99×10^9
1,2,4-trimethylbenzene (**5**)	1.92	TCA	2.36	0.055	8.59×10^9
1,2,3,4-tetramethylbenzene (**6**)	1.84	TCA	2.28	0.042	1.14×10^{10}
1,2,3,5-tetramethylbenzene (**7**)	1.83	TCA	2.27	0.041	1.17×10^{10}
5,8-dimethyltetrahydronaphthalene (**8**)	1.81	TCA	2.25	0.040	1.20×10^{10}
durene (**9**)	1.78	TCA	2.22	0.041	1.17×10^{10}
octahydrophenanthrene (**10**)	1.77	TCA	2.21	0.037	1.30×10^{10}
octahydroanthracene (**11**)	1.72	TCA	2.16	0.034	1.42×10^{10}
pentamethylbenzene (**12**)	1.71	TCA	2.15	0.035	1.38×10^{10}
hexamethylbenzene (**13**)	1.59	TCA	2.03	0.031	1.56×10^{10}

[a] Oxidation potentials from square-wave voltammetry measurements (see Experimental Section) in methylene chloride–trifluoroacetic acid–trifluoroacetic anhydride (45:5:1) at a platinum ultramicroelectrode, using ferrocene as internal standard, converted to *V* vs SCE according to E(SCE) = E(ferrocene) + 0.44 V. For the compounds **1**–**4** $E^{o\prime}$ values (vs SCE) from ref 15 were used. [b] Calculated according to eq 2; E^{red}DCA = −0.91 V, E^{red}_{TCA} = −0.44 V.

of maximum absorption, estimates of 65 600 at 530 nm and 45 000 at 715 nm are obtained for $DMS^{\bullet+}$ and $TAA^{\bullet+}$ by comparison with the signal from the $TTA^{\bullet+}$.[10] In principle, the extinction coefficient of any radical cation that absorbs appreciably in the visible region can be obtained by the DCA/biphenyl secondary electron transfer method, if the oxidation potential of the neutral species is lower than that of neutral biphenyl by at least 220 mV, so that reverse electron transfer to re-form the biphenyl radical cation is not important. Radical cations of donors with higher oxidation potentials could be studied by using TCA as the excited-state acceptor since in this case a more oxidizing primary radical cation such as *m*-xylene can be formed.

B. Free-Ion Yields. Pulsed laser excitation of a solution of DCA in the presence of 0.15 M biphenyl and 5×10^{-4} M TTA at 367 nm, and of a solution of benzophenone in benzene of identical optical density at 367 nm, results in the formation of absorbances due to $TTA^{\bullet+}$ at 670 nm and the triplet state of benzophenone at 525 nm,[11] respectively. The quantum yield for free-ion formation in the DCA/biphenyl system can be obtained by comparing the signal sizes due to the $TTA^{\bullet+}$ and the benzophenone triplet. Using the literature value of 7220 for the extinction coefficient of benzophenone triplet at 525 nm,[11] assuming a quantum yield of unity for its formation, and taking a value for the extinction coefficient of $TTA^{\bullet+}$ of 26 200 at 668 nm[10] yields a value of 0.72 for Φ_{sep} for the DCA/0.15 M biphenyl system.

The solution of DCA with 0.15 M biphenyl can thus be used as an actinometer for the quantum yields of free radical ions, which are formed when the other donors are used to quench the excited states of DCA and TCA. For most of the experiments DMS was used as the free-ion monitor due to the fact the extinction coefficient of the radical cation of this species was larger than those of the radical cations of the other monitors. Absolute quantum yields for free-ion formation for quenching of both TCA and DCA by all of the donors of Chart I in the presence of 5×10^{-4} M DMS were obtained by comparison of the $DMS^{\bullet+}$ optical densities with that obtained for the DCA/biphenyl system. The measurements of the transient optical densities were obtained by integrating over the optical density vs time wave form for 1 μs, starting 400 ns after the laser pulse. Because the extinction coefficient of the DMS radical cation is large, low laser energies could be used (<1 mJ) and small concentrations of the radical ion could easily be detected ($< 5 \times 10^{-6}$ M), and thus decay of the radical cation via second-order diffusive electron recombination reactions with the corresponding radical anion was not important. The concentrations of the donors were ca. 0.05 M. For each solution, the extent of quenching of the fluorescence of the cyanoanthracene was measured by steady-state emission spectroscopy, and the free-ion quantum yields were corrected for the incomplete interception of the excited-state singlets. In general, the fluorescence quenching was more than 90% complete. By use of these donors with the two acceptors, free-ion yields for 22 different ion pairs were thus obtained (Table II). A large difference is observed between the free-ion quantum yield for the ion pair with the largest value of $-\Delta G_{-et}$, the reaction exothermicity (vide infra), (1,2,4-trimethylbenzene/DCA, Φ_{sep} = 0.392) and that with the smallest

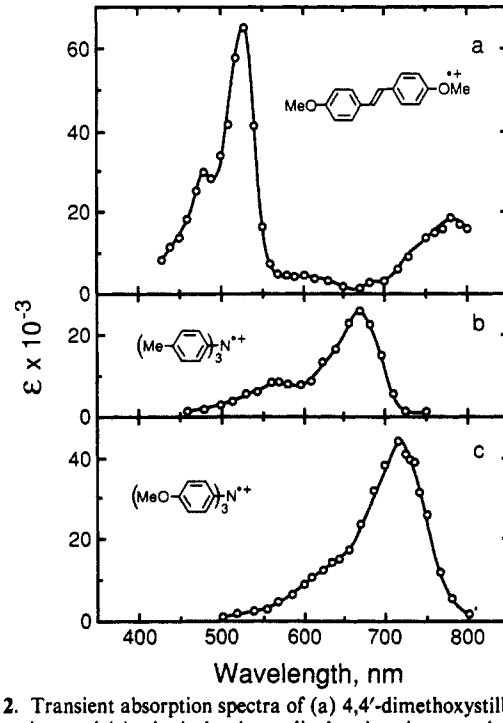

Figure 2. Transient absorption spectra of (a) 4,4′-dimethoxystilbene, (b) tritolylamine, and (c) trianisylamine radical cations in acetonitrile solution, all in the presence of oxygen as a DCA radical-anion scavenger.

(11) Carmichael, I.; Hug, G. L. *J. Phys. Chem. Ref. Data* **1986**, *15*, 1.

Table III. Quantum Yields for Free Radical Ion Formation and Rate Constants for Return Electron Transfer For Radical-Ion Pairs of Cyanoanthracene Radical Anions and Substituted "Two-Ring" Radical Cations

radical cation	E^{ox}_D,[a] V (vs SCE)	radical anion	$-\Delta G_{-et}$,[b] eV	Φ_{sep}	k_{-et}, s^{-1}
biphenyl (**14**)	1.96	DCA	2.87	~0.83[c]	$\sim 1.0 \times 10^8$
3,3'-dimethylbiphenyl (**15**)	1.85	DCA	2.76	0.62	3.06×10^8
naphthalene (**16**)	1.80	DCA	2.71	0.58[d]	3.62×10^8
fluorene (**17**)	1.71	DCA	2.62	0.49	5.20×10^8
2-methylnaphthalene (**18**)	1.68	DCA	2.59	0.43[d]	6.63×10^8
4,4'-dimethylbiphenyl (**19**)	1.66	DCA	2.57	0.37	8.51×10^8
2,6-dimethylnaphthalene (**20**)	1.59	DCA	2.50	0.32[d]	1.06×10^9
biphenyl (**14**)	1.96	TCA	2.40	0.24	1.58×10^9
3,3'-dimethylbiphenyl (**15**)	1.85	TCA	2.29	0.15	2.83×10^9
naphthalene (**16**)	1.80	TCA	2.24	0.12	3.67×10^9
fluorene (**17**)	1.71	TCA	2.15	0.083	5.52×10^9
2-methylnaphthalene (**18**)	1.68	TCA	2.12	0.072	6.44×10^9
4,4'-dimethylbiphenyl (**19**)	1.66	TCA	2.10	0.066	7.08×10^9
2,6-dimethylnaphthalene (**20**)	1.59	TCA	2.03	0.059	7.97×10^9

[a] Oxidation potentials from square-wave voltammetry measurements (see Experimental Section) in methylene chloride–trifluoroacetic acid–trifluoroacetic anhydride (45:5:1) at a platinum ultramicroelectrode, using ferrocene as internal standard, converted to V vs SCE according to E(SCE) = E(ferrocene) + 0.44 V. [b] Calculated according to eq 2; $E^{red}_{DCA} = -0.91$ V, $E^{red}_{TCA} = -0.44$ V. [c] The measured Φ_{sep} is 0.75 after extrapolation to zero concentration. However, in this case, relatively strong exciplex emission is observed, and we estimate that formation of the solvent-separated radical ion pair is only ca. 90% efficient. [d] An additional error of ±5% is associated with the values for these donors with DCA due to the concentration dependence of the free-ion quantum yields, which result from interception of the intermediate exciplexes and ion pairs by the donors (ref 19). The quantum yields reported here are those obtained by extrapolation to zero donor concentration.

Table IV. Quantum Yields for Free Radical Ion Formation and Rate Constants for Return Electron Transfer For Radical-Ion Pairs of Cyanoanthracene Radical Anions and Substituted-Phenanthrene "Three-Ring" Radical Cations

radical cation	E^{ox}_D,[a] V (vs SCE)	radical anion	$-\Delta G_{-et}$,[b] eV	Φ_{sep}	k_{-et}, s^{-1}
phenanthrene (**21**)	1.73	DCA	2.64	0.62[c]	3.06×10^8
2-methylphenanthrene (**22**)	1.67	DCA	2.58	0.56[c]	3.93×10^8
3,6-dimethylphenanthrene (**23**)	1.52	DCA	2.43	0.32[c]	1.06×10^9
phenanthrene (**21**)	1.73	TCA	2.17	0.156	2.71×10^9
2-methylphenanthrene (**22**)	1.67	TCA	2.11	0.120	3.67×10^9
3,6-dimethylphenanthrene (**23**)	1.52	TCA	1.96	0.062	7.56×10^9

[a] Oxidation potentials from square-wave voltammetry measurements (see Experimental Section) in methylene chloride–trifluoroacetic acid–trifluoroacetic anhydride (45:5:1) at a platinum ultramicroelectrode; ferrocene as internal standard, converted to V vs SCE according to E(SCE) = E(ferrocene) + 0.44 V. [b] Calculated according to eq 2; $E^{red}_{DCA} = -0.91$ V, $E^{red}_{TCA} = -0.44$ V. [c] An additional error of ±5% is associated with the values for these donors with DCA due to the concentration dependence of the free-ion quantum yields, which result from interception of the intermediate exciplexes and ion pairs by the donors (ref 19). The quantum yields reported here are those obtained by extrapolation to zero donor concentration.

ΔG_{-et} (hexamethylbenzene/TCA, $\Phi_{sep} = 0.031$). For several of the donors with TCA as the acceptor, the free-ion quantum yields, corrected for the different amounts of incomplete interception, were found to depend upon the donor concentration. In all cases a decrease in quantum yield was observed as a function of increasing donor concentration. The quantum yields summarized in Table II are those obtained by extrapolating the quantum yields to zero concentration of the donor. We have attributed this decrease in quantum yield with concentration to the formation of ground-state CT complexes. It has been noted previously that quantum yields of free-ion formation may be different for irradiation of free donor/acceptor systems and the corresponding ground-state CT complexes.[12]

Summarized in Tables III and IV are the quantum yields obtained with the two-ring and three-ring donors. For several of these donors, concentration-dependent quantum yields were found for ion pairs not only of $TCA^{\bullet-}$ but also of $DCA^{\bullet-}$. In this case, interception of the ion pairs by the neutral donors occurs to form pairs in which the cations are present as dimers, which can decrease the quantum yield. The quantum yield data in Tables III and IV are values obtained by extrapolation to zero donor concentration. A full kinetic analysis of the mechanisms of these concentration-dependent quantum yields will be provided elsewhere.

The relative transient optical densities obtained were found to be reproducible to within ±5% for solutions that were repeatedly compared several months apart. The absolute quantum yields for free-ion formation, however, depend upon the extinction coefficients of the benzophenone triplet and the tritolylamine radical cation. The errors in the quantum yields are thus determined by the errors in the extinction coefficients, which are difficult to estimate (for example, see ref 11). However, experiments have been performed in which Φ_{sep} were obtained for quenching of the excited state of *N*-methylacridinium with several

(12) (a) Ledwith, A. In *The Exciplex*; Gordon, M., Ware, W. R., Eds.; Academic Press: New York, 1975; p 209. (b) Jones, G., II In *Photoinduced Electron Transfer*; Fox, M. A., Chanon, M., Eds.; Elsevier: Amsterdam, 1988; Part A, Chapter 1.7. (c) Mataga, N.; Kanda, Y.; Okada, T. *J. Phys. Chem.* **1986**, *90*, 3880.

(13) (a) Weller, A. *Z. Phys. Chem. (Wiesbaden)* **1982**, *130*, 129. (b) Schulten, K.; Staerk, H.; Weller, A.; Werner, H.-J.; Nickel, B. *Z. Phys. Chem. (Frankfurt am Main)* **1976**, *101*, 371. (c) Werner, H.-J.; Staerk, H.; Weller, A. *J. Chem. Phys.* **1978**, *68*, 2419.

(14) Knibbe, H.; Rehm, D.; Weller, A. *Ber. Bunsenges. Phys. Chem.* **1968**, *72*, 257.

(15) Howell, J. O.; Goncalves, J. M.; Amatore, C.; Klasinc, L.; Wightman, R. M.; Kochi, J. K. *J. Am. Chem. Soc.* **1984**, *106*, 3968.

(16) (a) Weller, A. *Z. Phys. Chem. (Wiesbaden)* **1982**, *133*, 93. (b) Weller, A. *Pure Appl. Chem.* **1982**, *54*, 1885.

(17) Gould, I. R.; Moody, R.; Farid, S. *J. Am. Chem. Soc.* **1988**, *110*, 7242.

(18) Knibbe, H.; Röllig, K.; Schäfer, F. P.; Weller, A. *J. Chem. Phys.* **1967**, *47*, 1184.

(19) Details of the spectroscopy and dynamics of the exciplexes formed between the cyanoanthracenes and the one-ring and two-ring donors in nonpolar and polar solvents will be reported separately.

(20) (a) Hopfield, J. J. *Proc. Natl. Acad. Sci. U.S.A.* **1974**, *71*, 3640. (b) Van Duyne, R. P.; Fischer, S. F. *Chem. Phys.* **1974**, *5*, 183. (c) Ulstrup, J.; Jortner, J. *J. Chem. Phys.* **1975**, *63*, 4358. (d) Siders, P.; Marcus, R. A. *J. Am. Chem. Soc.* **1981**, *103*, 741, 748. (e) Brunschweig, B. S.; Logan, J.; Newton, M. D.; Sutin, N. *J. Am. Chem. Soc.* **1980**, *102*, 5798.

(21) (a) Marcus, R. A. *J. Chem. Phys.* **1956**, *24*, 966. (b) Marcus, R. A. *Annu. Rev. Phys. Chem.* **1964**, *15*, 155.

of the simple substituted benzenes of Chart I as donors, using both the transient absorption technique and also using pulsed photoacoustic spectroscopy. Although this latter method uses a different actinometer, very similar values were obtained for Φ_{sep}.[5c] We thus estimate that the absolute free-ion quantum yields are accurate to ±10%, although the errors in the relative quantum yields are smaller. If all of the quantum yields are actually smaller than the values in the Tables II–IV by 10%, then the changes in the best values of the parameters required to fit the electron-transfer rate data (vide infra) are actually less than 10%. The quantum yield data summarized in Tables II and III for the one-ring and two-ring data are in some cases slightly different from our previously published values (ref 5, 17, and 22). The differences are a consequence of further refinement of the data due to repeated measurements, and more quantitative analysis of the concentration-dependent quantum yields, to be described separately.

The relative quantum yields were found to depend upon the laser excitation energy for excitation energies greater than 5 mJ cm^{-2}. The high extinction coefficient of the monitor radical cations, however, and the extensive use of signal averaging allowed easy determination of accurate optical densities using conditions of ca. 1 mJ cm^{-2}, and usually energies lower than this were used so that laser intensity effects were not important. The origin of the laser intensity effect has not been investigated.

C. Electron-Transfer Rates. By use of the quantum yield data summarized in Tables II–IV, rates of return electron transfer (k_{-et}, Scheme I) can be obtained with eq 1 if k_{sep} is known. A value for k_{sep} has been obtained from studies in which DCA- and TCA-photoinitiated electron-transfer oxidations of diphenylethylene and phenylacetylene led to different chemical products from the geminate radical-ion pair and the free radical ions.[4] From quenching studies in which the ratio of the quantum yields of these two products was compared, estimates were made of the lifetimes of the ion pairs. In this manner a value of ca. 5×10^8 s^{-1} was obtained for k_{sep}.[4] Weller has also obtained a value of 5×10^8 s^{-1} from studies of the effects of external magnetic fields on the dynamics of the radical-ion pair formed between dimethylaniline and pyrene.[13] We thus conclude that the structural effects on this rate are small for organic radical ions in acetonitrile solution. At a minimum we can assume that this rate is a constant for radical-ion pairs in which the structural differences among the anions and cations are small, as in the present case. Values for k_{-et} are thus obtained from the Φ_{sep}, (Tables II–IV) and eq 1 by assuming a constant value for k_{sep} of 5×10^8 s^{-1} for all of the ion pairs. It is clear that the rates of the return electron transfer reaction vary over a wide range, and that the rates are smallest for those reactions in which the return electron transfer is most exothermic (i.e., ΔG_{-et} is most negative).

D. Determination of ΔG_{-et}. The return electron transfer free energy changes were calculated by using eq 2, in which E^{red}_A and

$$\Delta G_{-et} = E^{red}_A - E^{ox}_D \qquad (2)$$

E^{ox}_D are the reduction potential of the acceptor and the oxidation potential of the donor, respectively. Such equations often include a Coulomb term,[14] which accounts for the stabilization of the ion pair compared to the free ions due to the proximity of oppositely charged ions. However, for the solvent-separated ion pairs in which the distance between the charges is ca. 7–8 Å, this Coulombic stabilization *in acetonitrile*, amounts to only ca. 55 mV.[14] Furthermore, since the solvent-separated pair is likely to be slightly less solvated and thus less stabilized than the free radical ions, the difference in energy between the solvent-separated and free radical ions could be even less than 55 mV. The Coulomb term is thus considered to be negligible compared to the overall magnitude of the ΔG_{-et}.

Reversible electrochemical reduction potentials of −0.91 and −0.44 V vs SCE were measured in acetonitrile for DCA and TCA. Although electrochemical oxidation in acetonitrile of most of the donors used in this study is not reversible,[15] reversible or semi-reversible oxidation potentials could be obtained by using square-wave voltammetry (see Experimental Section) for the one aromatic ring compounds **5–13** and for the alkylated two- and three-ring compounds (Tables II–IV) in a methylene chloride–trifluoroacetic acid–trifluoroacetic anhydride (45:5:1) solvent mixture. Even under these conditions, however, oxidation of the one aromatic ring donors **1–4** was irreversible. The electrochemical oxidation of many of the one-ring donors has been studied previously by Amatore and Kochi et al.,[15] who reported reversible oxidation potentials in trifluoroacetic acid. The measurements of the reversible oxidation potentials of the donors **5–7**, **9**, **12**, and **13** made by Amatore and Kochi agree with our square-wave voltammetry measurements within 50 mV. Thus, for the donors **5–13** the square-wave voltammetry oxidation potentials in the methylene chloride solvent were used for E^{ox}_D, and for the donors **1–4**, the oxidation potentials reported by Amatore and Kochi were used. Electrochemical oxidation of the unsubstituted donors biphenyl, naphthalene, and phenanthrene was irreversible with square-wave voltammetry. However, a value for the E^{ox}_D of naphthalene was obtained by using a transient absorption technique in which the equilibrium constant (K) for process 3 was

$$N^{\cdot+} + D \overset{K}{\rightleftharpoons} N + D^{\cdot+} \qquad (3)$$

determined by monitoring the equilibrium concentration of naphthalene radical cation ($N^{\cdot+}$) at 680 nm[8] in the presence of a known concentration of a donor D. Values for K were 2.4 and 0.24, respectively, when durene and 1,2,3,5-tetramethylbenzene were used as the donors. Using the values of E^{ox}_D given in Table II for these two donors gives an average value of 1.80 V vs SCE for E^{ox}_D for naphthalene, which is identical with the electrochemical oxidation potential obtained in the methylene chloride solvent mixture. Because of the good agreement between the irreversible oxidation potential of naphthalene from the square-wave voltammetry, and the directly measured E^{ox}_D in acetonitrile from the transient absorption experiment, we used the methylene chloride electrochemical oxidation potentials for E^{ox}_D, for all of the two- and three-ring donors.

Finally, we had to determine whether the oxidation potentials in the methylene chloride solvent mixture are generally appropriate for the calculation of ΔG_{-et} in acetonitrile. By use of square-wave voltammetry, semireversible oxidation potentials were measured in acetonitrile for the compounds with the most stable radical cations. Thus, for hexamethylbenzene (**13**), 2,6-dimethylnaphthalene (**20**), and 3,6-dimethylphenanthrene (**23**), $(E^{ox})_{CH_3CN}$ of 1.63, 1.62, and 1.55 V vs SCE were obtained, respectively. These potentials are only 30–40 mV more positive than the values measured in the methylene chloride solvent mixture (Tables II–IV). This difference was neglected both because it is small compared to the absolute values of ΔG_{-et} and because it is in the opposite direction to the Coulombic term of ca. 50 mV, which was also neglected. The absolute values of ΔG_{-et} are estimated to be subject to an error of ±60–70 mV, although the errors in the differences between the ΔG_{-et} values for ion pairs from any of the sets of donors are considerably smaller (Tables II–IV). Several of the ΔG_{-et} values given in the tables are slightly different from our previously published values (ref 5, 17, and 22) as a consequence of further refinement of the electrochemical data after repeated measurements.

IV. Discussion

A. Nature of the Ion Pair. The reaction Scheme I indicates that electron transfer (k_{et}) takes place to form a geminate radical-ion pair. In principle, one can consider the intermediacy of two such species, namely, a contact ion pair and a solvent-separated ion pair.[2,16] The major differences between these two species is the higher electronic coupling in the contact pair compared to the solvent-separated pair, and the higher solvation of the latter species compared to the former.[17] The higher electronic coupling in the contact ion pairs leads to a significant probability for emission from these species, and also for mixing of ion-pair character with locally excited state character, and indeed these species are the

(22) Gould, I. R.; Farid, S. *J. Am. Chem. Soc.* **1988**, *110*, 7883.

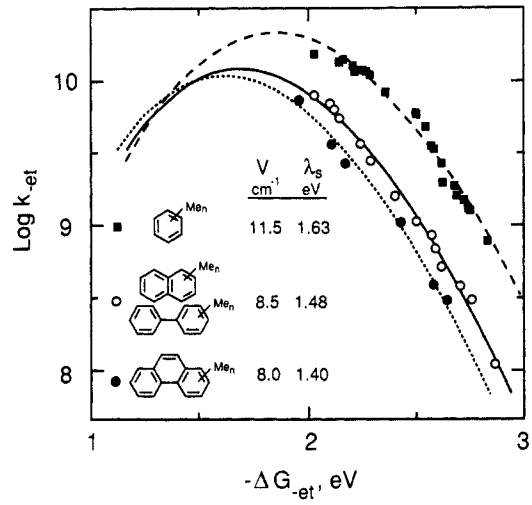

Figure 3. Plots of log return electron transfer rate constant (k_{-et}) vs reaction free energy (ΔG_{-et}) for radical-ion pairs of 9,10-dicyanoanthracene and 2,6,9,10-tetracyanoanthracene radical anions with the one-ring, two-ring, and three-ring donor radical cations. The lines through the points represent fits to eq 4 with the values for V and λ_s indicated in the figure, and using 0.25 eV and 1500 cm^{-1} for λ_v and ν, respectively.

commonly encountered exciplexes in organic photochemistry.[2,16] In the current solvent, acetonitrile, exciplex emissions are rarely observed, however. This lack of emission is usually attributed to rapid dissociation of the initially formed contact ion pairs into solvent-separated ion pairs, or it has been suggested that, in polar solvents such as acetonitrile, the electron-transfer quenching results in the formation of the solvent-separated ion pair directly.[18] We have observed weak exciplex emissions upon quenching of the first singlet state of DCA in acetonitrile using several of the donors. In each case, lifetime measurements indicate that the only process of significance for these exciplexes is solvation to form the solvent-separated radical-ion pairs.[19] In the case of TCA, which is much easier to reduce than DCA, we were not able to detect any exciplex emission in acetonitrile in the presence of the donors mentioned in this work. The species that is responsible for the energy-wasting return electron transfer in these systems is thus assigned to the solvent-separated pair. The solvent-separated pairs are assumed to have a structure in which each ion is fully solvated, with a layer of solvent molecules between the ions, and the ions are assumed to be in a state of motion in which the relative orientation and inter-ion distance are not constant.

B. Analysis of Electron-Transfer Rates. In Figure 3 are shown plots of log k_{-et} vs ΔG_{-et} for all three sets of donors. The plots show that for each set (one-ring, two-ring, or three-ring) there is very little scatter, which supports the assumption that the separation rate is a constant for each radical ion pair set. In addition it is clear that the data for the ion pairs of DCA cannot be distinguished from those of TCA. However, a clear distinction can be made between the ion pairs with the one-ring and two-ring donors, and a smaller distinction between the two-ring and three-ring donors. From these observations we conclude that the structural differences within each set of ion pairs are small and that the size of the aromatic nucleus of the donor has an influence on the return electron transfer rates. The fact that the rates measured with the donors **8**, **10**, and **11** are indistinguishable from those of the other one-ring donors demonstrates that it is the size of the aromatic nucleus that is important, and not the overall molecular size.

The most unusual aspect of the data is that the electron-transfer rates decrease as the reaction exothermicities ($-\Delta G_{-et}$) increase. In order to explain this observation, we must turn to the theories of electron-transfer reactions. Modern theories treat electron transfer as a radiationless transition and cast the rate in a golden rule type expression in which the rate is given as the product of an electronic matrix element squared (V^2) and a Franck–Condon weighted density (FCWD) of states (eq 4a).[20] The Franck–

$$k_{-et} = (2\pi/\hbar)|V|^2\mathrm{FCWD} \quad (4a)$$

$$k_{-et} = (\pi/\hbar^2\lambda_s k_b T)^{1/2}|V|^2 \sum_{w=0}^{\infty}(e^{-s}S^w/w!)\exp\{-[(\lambda_s + \Delta G + wh\nu)^2/4\lambda_s k_b T]\} \quad (4b)$$

$$S = \lambda_v/h\nu \quad (4c)$$

Condon term contains the dependence on the reaction exothermicity ($-\Delta G_{-et}$). The rearranged modes related to the solvent reorganization energy (λ_s) are treated classically. The vibrational modes associated with λ_v are treated quantum mechanically and it is assumed that the frequencies of these modes can be represented by a single averaged frequency ν. Although somewhat less appealing than the classical descriptions of Marcus,[21] eq 4 reproduces the essential elements of the classical theory, including the prediction of a decrease in rate with increasing exothermicity (the Marcus inverted region), for reactions that are more exothermic than the sum of λ_s and λ_v (the total reorganization energy). Equation 4 also has the advantage of providing a quantitative distinction between solvent and vibrational reorganization energies and provides a basis for the interpretation of observations such as the effect of isotopic substitution on electron-transfer rates.[22] The data shown in Figure 3 represent a clear example of the Marcus inverted region.

C. Fitting Parameters. A curve-fitting procedure is required to find the best values of the parameters V, λ_s, λ_v, and ν to fit the data using eq 4. Clearly, more than one set of parameters can be found to fit each set of data, and in order to make the problem more tractable, we have attempted to restrict the number of variable parameters. The differences between the classical Marcus theory and the semiclassical theory are most pronounced in the inverted region. For larger contributions of λ_v to the total reorganization energy, or for larger values of ν, eq 4 predicts a smaller rate of decrease in k_{-et} in the inverted region. We have chosen a fixed value of 1500 cm^{-1} for ν. This is a typical value for carbon–carbon skeletal vibrations and is also that used by Closs and Miller[23] in their study of intramolecular electron transfer in rigid donor/acceptor systems, which provides the best data to compare with our own. Although we have observed that substitution of deuterium for hydrogen affects the rates of electron transfer in these radical-pair systems,[22] we still believe that a frequency smaller than the 3000 cm^{-1} suggested by the isotope experiments represents the best *average* of the rearranged vibrational modes.

1. Vibrational Reorganization Energy (λ_v). Preliminary curve fitting clearly indicates that λ_v must be significantly smaller than λ_s in order to obtain a good fit of the theoretical curve to the data. Good fits to the two-ring data can be obtained for values of λ_v of less than or equal to 0.6 eV,[5a] and for the one-ring data, values less than or equal to 0.3 eV have to be used.[5b] This is entirely consistent with expectation for internal reorganization energies of organic molecules, which are usually considered to be small, or are even ignored,[24] except under unusual circumstances.[25] An estimate for λ_v can be obtained from semiempirical molecular orbital calculations using a method similar to that described by Nelsen.[25b] A potential energy diagram for electron transfer within a donor/acceptor pair is shown in Figure 4, in which the horizontal axis represents change in position (reorganization) of the nuclei of the species undergoing reaction and, in the general case, of the nuclei of the solvent. The reorganization energy (λ) for the return electron transfer from the ion-pair state ($A^{\bullet+}D^{\bullet+}$) to the neutral

(23) (a) Closs, G. L.; Johnson, M. D.; Miller, J. R.; Piotrowiak, P. *J. Am. Chem. Soc.* **1989**, *111*, 3751. (b) Closs, G. L.; Miller, J. R. *Science* **1988**, *240*, 440. (c) Closs, G. L.; Calcaterra, L. T.; Green, N. J.; Penfield, K. W.; Miller, J. R. *J. Phys. Chem.* **1986**, *90*, 3673. (d) Miller, J. R.; Calcaterra, L. T.; Closs, G. L. *J. Am. Chem. Soc.* **1984**, *106*, 3047. (e) Calcaterra, L. T.; Closs, G. L.; Miller, J. R. *J. Am. Chem. Soc.* **1983**, *105*, 670.

(24) (a) Marcus, R. A. *J. Chem. Phys.* **1957**, *26*, 872. (b) Eberson, L. In *Advances in Physical Organic Chemistry*; Gold, V., Bethell, D., Eds.; Academic: London, 1982; Vol. 18, p 79.

(25) (a) Nelsen, S. F.; Blackstock, S. C.; Haller, K. J. *Tetrahedron* **1986**, *42*, 6101. (b) Nelsen, S. F.; Blackstock, S. C.; Kim, Y. *J. Am. Chem. Soc.* **1987**, *109*, 677.

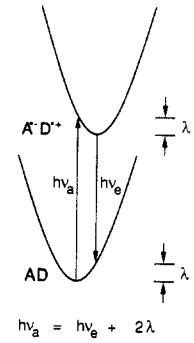

Figure 4. Potential energy surfaces for a contact radical-ion pair ($A^{\bullet-}D^{\bullet+}$) and the neutral donor and acceptor (AD) showing the relationship between the charge-transfer absorption, charge-transfer emission, and reorganization energies. In the gas phase, or in nonpolar solvents, the reorganization energy, λ, is assumed to be equal to the internal vibrational component, λ_v (see text). The difference between the charge-transfer absorption and emission energies is equal to twice the reorganization energy if the same, symmetrical functions describe the potential energy surfaces of both $A^{\bullet-}D^{\bullet+}$ and AD.

state (AD) is given by the difference in the energy between AD in its equilibrium nuclear geometry and AD in the equilibrium nuclear geometry of $A^{\bullet-}D^{\bullet+}$ (Figure 4). In the gas phase (the conditions of the calculation), this reorganization energy is equal to the internal vibrational reorganization energy, λ_v. Energies and geometries for several of the molecules and radical ions studied here have been obtained with the semiempirical MOPAC package (see Experimental Section). For any ion pair, the difference in the heat of formation of the acceptor in its equilibrium nuclear geometry and in the equilibrium nuclear geometry of the radical anion is added to the corresponding difference in the heats of formation for the donor. The sum of these energy differences is then taken as an estimate for λ_v for the return electron transfer reaction for that pair. The energy difference for DCA in the two geometries is calculated to be 0.09 eV. The calculations provide a remarkably constant value for the corresponding energy differences of the donors **2**, **4**, **5**–**7**, **9**, **12**, and **13**, the two-ring donor **18** and the three-ring donor **21**, of 0.15 ± 0.02 eV. The total averaged reorganization energy obtained by adding the reorganization energies of the acceptor and the donors is thus 0.24 ± 0.02 eV.[26] Although the errors associated with the calculations are not known, the results support the assumption that λ_v is indeed small, and that this parameter is a constant for all of the ion pairs of the present study.

An experimental estimate for λ_v can also be obtained. The energy difference between the charge-transfer absorption ($h\nu_a$) and emission ($h\nu_e$) energies, illustrated in Figure 4, is equal to twice the reorganization energy (eq 5) if the two potential energy

$$h\nu_a - h\nu_e = 2\lambda \qquad (5)$$

surfaces are the same and symmetrical.[26] Although these radiative processes cannot be observed for the solvent-separated radical-ion pairs due to weak electronic coupling, for donors and acceptors in contact, both charge-transfer absorption and charge-transfer (exciplex) emission are well-known.[27] In a highly nonpolar solvent, the reorganization energy is dominated by the internal vibrational component (i.e., λ_s is negligible compared to λ_v). Thus, we assume that a reorganization energy obtained with eq 5 in a nonpolar solvent such as cyclohexane is equal to the vibrational reorganization energy, λ_v, which should be identical for the contact and solvent-separated radical-ion pairs studied here. Both charge-transfer absorption and emission can be observed for the TCA/hexamethylbenzene contact pair in cyclohexane. In Figure 5 is shown the charge-transfer (exciplex) emission spectrum (λ_{max} = 584 nm) of TCA (ca. 2×10^{-6} M^{-1}) in the presence of 0.026 M hexamethylbenzene. The emission excitation spectrum, which is similar to the absorption spectrum of the solution, shows maxima due to the free TCA (A, eq 6) at 424 and 401 nm and, in addition, a broad charge-transfer absorption at longer wavelength due to the ground-state complex AD, eq 6. The absorption band of the

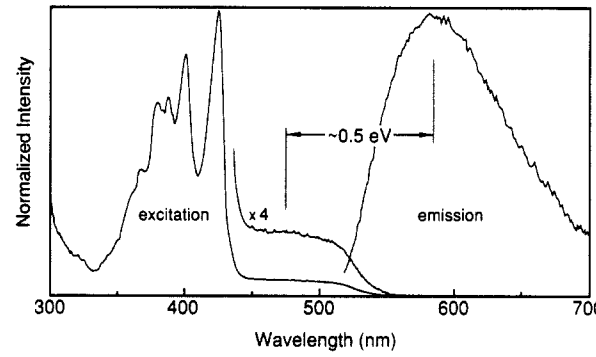

Figure 5. Charge-transfer emission, and emission excitation spectra for TCA (ca. 2×10^{-6} M) in cyclohexane in the presence of 0.026 M hexamethylbenzene. The residual monomer fluorescence has been subtracted from the emission spectrum. The energy difference between the charge-transfer emission and excitation spectra is equal to twice the charge-transfer reorganization energy (see text).

$$A + D \rightleftharpoons AD \qquad (6)$$

complex is not well resolved; however, the maximum is clearly centered at 475 ± 5 nm (Figure 5). An energy difference between absorption and emission of ~0.5 ± 0.03 eV is thus obtained, which yields a value for λ_v of 0.25 ± 0.02 eV. Similar experiments for the TCA/durene system in cyclohexane also give a reorganization energy of ca. 0.25 eV. The reorganization energy of 0.25 eV from the spectroscopy, which is close to the value of ca. 0.24 eV suggested by the MO calculations, is consistent with the small value for λ_v suggested by the preliminary curve fitting for the one-ring donors and is thus taken as a fixed value for λ_v for all of the radical-ion pairs.

2. Solvent Reorganization Energy (λ_s). The curve-fitting procedure thus involves finding the best values for V and λ_s that fit the data. With only two variable parameters, values for V and λ_s can be obtained with a higher degree of confidence. Obviously, different values of the parameters are required to fit the three sets of data, as indicated in Figure 3. In general, as the size of the aromatic nucleus of the radical cation in the pair decreases, a larger solvent reorganization energy is required for the best fit, from 1.40 eV for the three-ring donors to 1.63 eV for the one-ring donors. A larger value for the electronic coupling matrix element is also required as the size of the aromatic ring decreases (from 8.0 cm^{-1} for the three-ring to 11.5 cm^{-1} for the one-ring donors). The differences in these parameters between the two-ring and three-ring cations are small, however, which indicates that the size effect quickly saturates. The values of V and λ_s given in Figure 3 represent the best fits to each set of data. However, other combinations of these two parameters also give reasonable fits. In general, variations in V of ±1 cm^{-1}, with corresponding variations in λ_s of ∓0.05 eV, still lead to reasonable fits for each set of data. The best-fit values given here are not the same as those given in our previous publications[5] due to the refined values of k_{-et} and ΔG_{-et}.

We expect that the positive charge on the radical cations of the one-ring donors will be more localized than that on the radical cations of the donors with the larger rings. This will presumably result in somewhat higher solvation of the radical cations in the one-ring case, and thus a higher solvent reorganization energy. This same size effect is evident in the exciplex emission spec-

(26) The reorganization energy for the reaction AD → $A^{\bullet-}D^{\bullet+}$, is given by the corresponding energy difference for the ion-pair state. If the same symmetrical function is used to describe the potential energy surfaces of the two states, then the reorganization energy of this reaction is identical with that of the return electron transfer reaction, as indicated in Figure 4. In fact, identical parabolic functions are often used.[21] The reorganization energy for the reaction AD → $A^{\bullet-}D^{\bullet+}$, obtained by the MO method described in the text, is 0.22 ± 0.02 eV. Thus, the reorganization energies of the two reactions are very similar, which is consistent with the two potential energy surfaces of Figure 4 being similar.

(27) (a) Mulliken, R. S.; Pearson, W. B. *Molecular Complexes: A Lecture and Reprint Volume*; Wiley-Interscience: New York, 1969. (b) Weller, A. In *The Exciplex*; Gordon, M., Ware, W. R., Eds.; Academic Press: New York, 1975; p 23.

troscopy of the corresponding exciplexes. Although the solvent-separated pairs and the exciplexes (contact ion pairs) are solvated to significantly different degrees,[17] it is reasonable to expect that size effects on the solvation of these two species should be related. For exciplexes of the one-ring donors with DCA, a constant difference in emission energy of 0.49 ± 0.02 eV is observed between the nonpolar solvent cyclohexane and the polar acetonitrile. The corresponding energy difference for exciplexes of the two-ring donors with DCA is 0.35 ± 0.01 eV.[19] This suggests that the exciplex solvent stabilization energy is greater for the one-ring exciplexes than the two-ring exciplexes, which in turn suggests that the one-ring exciplexes are more highly solvated in the polar solvent, which is consistent with the larger value of λ_s for the one-ring donors.

Marcus has described a dielectric continuum model for λ_s as shown in eq 7, in which Δe is the transferred electronic charge,

$$\lambda_s = \frac{(\Delta e)^2}{4\pi\epsilon_0}\left(\frac{1}{d_A} + \frac{1}{d_{D^+}} - \frac{1}{R_{A^-D^+}}\right)\left(\frac{1}{n^2} - \frac{1}{\epsilon}\right) \qquad (7)$$

ϵ_0 is the permittivity of free space, n and ϵ are the solvent refractive index and dielectric constants, d_{A^-} and d_{D^+} are the diameters of the reduced acceptor and the oxidized donor, and $R_{A^-D^+}$ is their center-to-center separation.[21] Equation 7 was derived for spherical molecules and is thus difficult to apply in the present case, since the donors and acceptors are obviously not spherical. This is particularly a problem since the λ_s obtained from eq 7 are very sensitive to the values chosen for the diameters. However, eq 7 does predict that λ_s should increase if the diameter of either the donor or acceptor decreases. Since the effective radius of the radical cation clearly decreases with decreasing number of aromatic rings, eq 7 is at least consistent with the present observations.

The values for λ_s are larger than those reported for other electron-transfer reactions. For example, reorganization energies for self-exchange reactions of organic cations and anions in acetonitrile are typically of the order of 0.3–0.6 eV.[24b] However, the reactions described here are for solvent-separated radical-ion pairs rather than contact ion pairs. We have previously shown that the return electron transfer reactions within contact radical-ion pairs of TCA radical anions and the one-ring radical cations are characterized by a much smaller reorganization energy and a larger electronic coupling energy than the corresponding reactions of the solvent-separated ion pairs.[17] Indeed, the total reorganization energy obtained for the contact ion-pair reaction was ca. 0.8 eV, which is close to the reorganization energies for the self-exchange reactions. Thus, for reactions with small exothermicities such as exchange reactions, which are in fact isoenergetic ($\Delta G_{-et} = 0$), relatively fast electron transfer is expected when the radical-ion pairs are in contact due to the large electronic coupling and small reorganization energy under these conditions. For reactions with small exothermicities, slow electron transfer is expected if the radical-ion pairs are solvent separated because the reactions are not exothermic enough to overcome the large reorganization energy in this case. Conversely, for electron-transfer reactions with large exothermicities, relatively slow electron transfer is expected if the radical-ion pairs are in contact because the small reorganization energy that characterizes such reactions is insufficient to dissipate the energy stored in the ion pair (the inverted region effect). For electron-transfer reactions with large exothermicities, reaction within the solvent-separated radical-ion pair is relatively fast because the ion pair has sufficient energy to overcome the large reorganization energy in this case. Thus, we expect that the exchange reactions in a polar solvent such as acetonitrile should only occur when the reactants are in contact, which is consistent with the small reported reorganization energies for these reactions.

3. Electronic Coupling Matrix Elements (V). The coupling matrix element V is related to the orbital overlap integral, S_{AD},[28,29]

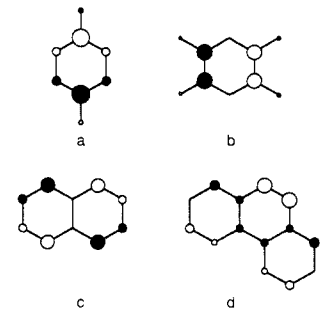

Figure 6. Singly occupied molecular orbitals for (a) *p*-xylene, (b) durene, (c) naphthalene, and (d) phenanthrene radical cations.

and in general we expect V to decrease as S decreases. Thus, larger molecules, which have more diffuse molecular orbitals and which are characterized by more complex nodal structures, should have somewhat lower orbital overlap, and hence smaller values of V.[30] This point is clearly illustrated in Figure 6 in which are shown the singly occupied molecular orbitals (SOMOs) of the *p*-xylene, durene, naphthalene, and phenanthrene radical cations, as obtained from the MOPAC calculations. The SOMOs of the substituted benzene radical cations are characterized by one of two types as illustrated by *p*-xylene and durene, although each has the same number of nodal planes. It is interesting that no distinction can be made between the return electron transfer kinetics of the ion pairs of the one-ring donors with the *p*-xylene-like SOMO and those with the durene-like SOMO. The electronic coupling seems only to distinguish between systems with differing overall sizes and degrees of nodal structure. The small values for V indicate rather weak coupling in these systems, which might be expected for the solvent-separated ion pairs. The electronic coupling is usually assumed to decrease exponentially with distance.[20] For the solvent-separated radical-ion pairs, we assume a center-to-center separation distance of ca. 7–8 Å.[14,17] For studies of electron transfer between free radical anions and neutral molecules in frozen glasses, Miller obtained values for V of ca. 300 cm^{-1} for 6-Å separation and ca. 30 cm^{-1} for 10-Å separation.[31] In their studies of electron transfer between donors and acceptors linked by rigid spacer groups, Closs and Miller obtained values of V which ranged from ca. 10 to 160 cm^{-1} for center-to-center distances of 11–6 Å.[23] In those cases, however, through-bond coupling plays an important role, as evidenced by the large stereoelectronic effects observed in those molecules.[23] Of the molecules studied by Closs and Miller, perhaps the most relevant to the present work is the species **24**. For this molecule,

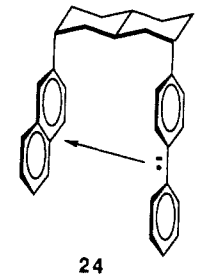

24

an electronic coupling matrix element of 58 cm^{-1} was obtained. The center-to-center distance of the donor and acceptor in this molecule is 6.2 Å. In this case, the stereochemical arrangement of the σ bonds should minimize the through-bond coupling, and the face-to-face geometry should enhance the through-space coupling.[23b] Compared to the structure **24**, the solvent-separated radical-ion pairs have a somewhat larger distance between the donor and acceptor, have a significantly "looser" structure, and,

(28) (a) Newton, M. D. *J. Phys. Chem.* **1986**, *90*, 3734. (b) Newton, M. D. *ACS Symp. Ser.* **1982**, *No. 198*, 255.
(29) Ohta, K.; Closs, G. L.; Morokuma, K.; Green, N. J. *J. Am. Chem. Soc.* **1986**, *108*, 1319.
(30) (a) Salem, L. *Electrons in Chemical Reactions*; Wiley: New York, 1982; p 239. (b) Brockelhurst, B. *J. Phys. Chem.* **1979**, *83*, 536. (c) Siders, P.; Cave, R. J.; Marcus, R. A. *J. Chem. Phys.* **1984**, *81*, 5613.
(31) (a) Miller, J. R.; Beitz, J. V.; Huddleston, R. K. *J. Am. Chem. Soc.* **1984**, *106*, 5057. (b) Miller, J. R.; Beitz, J. V. *J. Chem. Phys.* **1981**, *74*, 6476. (c) Miller, J. R.; Beitz, J. V. *J. Chem. Phys.* **1979**, *71*, 4579.

of course, have no through-bond interactions. Thus, compared to **24**, the low values of 8–11.5 cm^{-1} obtained for the electronic coupling in the ion pairs may be reasonable.

D. Comparison with Other Systems. As model systems for the study of the factors that control electron transfer rates, return electron transfers within geminate radical-ion pairs have the disadvantage that the donor/acceptor distance and orientation are not fixed compared to those systems in which the donor and acceptor are held between rigid spacer molecules.[23,32-35] Studies of systems in rigid media in which the donor/acceptor distances and orientations are fixed but not constant clearly show that electron transfer is nonexponential.[31,36] In this work it is assumed that a single averaged rate describes the return electron transfer process. Even if this assumption is not strictly valid, the kinetic model described here is appropriate in the absence of experimental evidence to the contrary and clearly represents a powerful predictive tool for free radical ion quantum yields. The radical-ion pair system has the considerable advantage that many different ion pairs with differing chemical properties can be easily prepared without chemical synthesis. In this manner we have been able to study several aspects of electron-transfer kinetics including the differences between contact and solvent-separated radical-ion pairs,[17] the differences between charge-shift and charge-recombination reactions,[5c] and the influence of isotopic substitution.[22]

There now exist several examples of the inverted region.[23,31,34,35,37-41] The results presented here and elsewhere for other radical ion pair systems[37-41] are significant because they demonstrate the importance of the inverted region for bimolecular electron-transfer reactions in homogeneous solution, whereas other studies in which the inverted region is observed have emphasized its importance in intramolecular reactions. Until the developments of recent years, the most famous test of the Marcus electron-transfer theory was the work of Rehm and Weller,[42] who showed that no inverted region could be observed for bimolecular electron-transfer quenching of excited states (k_{et}, Scheme I) even for very exothermic reactions. This observation has been explained variously as being due to the fact that these reactions are second order and become diffusion controlled when the electron transfer becomes very fast, and that for the very exothermic reactions, the initial electron transfer leads to the formation of excited states

Scheme II. Energy Diagram for Cosensitization Mechanism

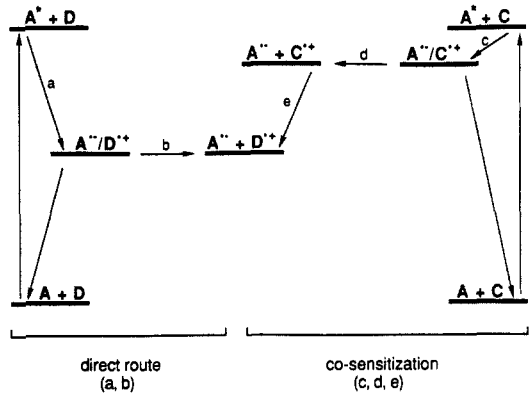

of the radical ions, or that other processes such as exciplex formation or proton transfer take place.[42,43] The main reason that the inverted region is observed clearly in the present systems is that the return electron transfer process, although bimolecular, is first order and does not require diffusive encounter of the donor and acceptor. In addition, the radical-ion pairs that were chosen do not undergo chemical reactions within the ion pairs and are structurally very similar. Finally, since the ion pairs are formed as a result of quenching of the lowest singlet states of the cyanoanthracenes, and since these are lower than the corresponding states of the donors, there are no electronic states of singlet multiplicity between the ion pairs and the neutral ground states. Population of the triplet state of the cyanoanthracenes would be energetically possible for most of the ion pairs studied here; however, this would require an intersystem-crossing step. For the solvent-separated radical-ion pairs the most probable intersystem-crossing mechanism would be that resulting from the hyperfine coupling between the electron and nuclear spins in the radical ions.[44] For the organic radical ions studied here, rates of intersystem crossing due to this mechanism are expected to be on the order of ca. 5×10^7 s^{-1} and would therefore not compete with the return electron transfer (ca. 10^8–10^{10} s^{-1}) and diffusive separation processes (5×10^8 s^{-1}).[44,45]

The radical-ion pairs thus represent a good system for the study of electron-transfer processes and indeed the inverted region has been observed in ion pairs by other groups.[37-41] Ohno et al. have observed return electron transfer in ion pairs formed as a result of quenching the MLCT state of ruthenium trisbipyridyl by amines.[41] Both the normal region and the inverted regions were observed in the return electron transfer; however, the data analysis in those systems is complicated by an intersystem-crossing step. Mataga[39] and Hasselbach[40] have measured rates of return electron transfer in organic radical-ion pairs. In those studies, somewhat scattered correlations were observed between the electron-transfer rates and the reaction exothermicities. This is undoubtedly due to the fact that the electron-transfer rates are highly susceptible to small changes in molecular structure, as evidenced by the differences between the one-ring, two-ring, and three-ring donors. Presumably the reason that a correlation with low scatter is observed in the present work is that the ion pairs are structurally very similar, and chemical reactions in the ion pair are not important. Another important feature of the present work is that the effects of radical ion pair self-quenching and ground-state

(32) Paddon-Row, M. N.; Oliver, A. M.; Warman, J. M.; Smit, K. J.; De Haas, M. P.; Oevering, H.; Verhoeven, J. W. *J. Phys. Chem.* **1988**, *92*, 6958. (b) Oevering, H.; Paddon-Row, M. N.; Heppener, M.; Oliver, A. M.; Cotsaris, E.; Verhoeven, J. W.; Hush, N. S. *J. Am. Chem. Soc.* **1987**, *109*, 3258. (c) Warman, J. M.; De Haas, M. P.; Oevering, H.; Verhoeven, J. W.; Paddon-Row, M. N.; Oliver, A. M.; Hush, N. S. *Chem. Phys. Lett.* **1986**, *128*, 95. (d) Warman, J. M.; De Haas, M. P.; Paddon-Row, M. N.; Cotsaris, E.; Hush, N. S.; Oevering, H.; Verhoeven, J. W. *Nature (London)* **1986**, *320*, 615.

(33) (a) Joran, A. D.; Leland, B. A.; Felker, P. M.; Zewail, A. H.; Hopfield, J. J.; Dervan, P. B. *Nature (London)* **1987**, *327*, 508. (b) Leland, B. A.; Joran, A. D.; Felker, P. M.; Hopfield, J. J.; Zewail, A. H.; Dervan, P. B. *J. Phys. Chem.* **1985**, *89*, 5571. (c) Joran, A. D.; Leland, B. A.; Geller, G. G.; Hopfield, J. J.; Dervan, P. B. *J. Am. Chem. Soc.* **1984**, *106*, 6090.

(34) Wasielewski, M. R.; Niemczyk, M. P.; Svec, W. A.; Pewitt, E. B. *J. Am. Chem. Soc.* **1985**, *107*, 1080.

(35) (a) Irvine, M. P.; Harrison, R. J.; Beddard, G. S.; Leighton, P.; Sanders, J. K. M. *Chem. Phys.* **1986**, *104*, 315. (b) Harrison, R. J.; Pearce, B.; Beddard, G. S.; Cowan, J. A.; Sanders, J. K. M. *Chem. Phys.* **1987**, *116*, 429. (c) Cowan, J. A.; Sanders, J. K. M.; Beddard, G. S.; Harrison, R. J. *J. Chem. Soc., Chem. Commun.* **1987**, 55.

(36) (a) Dorfman, R. C.; Lin, Y.; Zimmt, M. B.; Baumann, J.; Domingue, R. P.; Fayer, M. D. *J. Phys. Chem.* **1988**, *92*, 4258. (b) Dorfman, R. C.; Lin, Y.; Fayer, M. D. *J. Phys. Chem.* **1989**, *93*, 6388. (c) Lin, Y.; Dorfman, R. C.; Fayer, M. D. *J. Chem. Phys.* **1989**, *90*, 159.

(37) Levin, P. P.; Pluzhnikov, P. F.; Kuzmin, V. A. *Chem. Phys. Lett.* **1988**, *147*, 283.

(38) Kemnitz, K. *Chem. Phys. Lett.* **1988**, *152*, 305.

(39) Mataga, N.; Asahi, T.; Kanda, Y.; Okada, T.; Kakitani, T. *Chem. Phys.* **1988**, *127*, 249. (b) Mataga, N.; Kanda, Y.; Okada, T. *J. Phys. Chem.* **1986**, *90*, 3880. (c) Shiomaya, H.; Masuhara, H.; Mataga, N. *Chem. Phys. Lett.* **1982**, *88*, 161.

(40) Vauthey, E.; Suppan, P.; Haselbach, E. *Helv. Chim. Acta* **1988**, *71*, 93.

(41) (a) Ohno, T.; Yoshimura, A.; Mataga, N. *J. Phys. Chem.* **1986**, *90*, 3296. (b) Ohno, T. *J. Phys. Chem.* **1985**, *89*, 5709. (c) Ohno, T.; Yoshimura, A.; Shioyama, H.; Mataga, N. *J. Phys. Chem.* **1987**, *91*, 4365. (d) Ohno, T.; Yoshimura, A.; Mataga, N.; Tazuke, S.; Kawanishi, Y.; Kitamura, N. *J. Phys. Chem.* **1989**, *93*, 3546.

(42) Rehm, D.; Weller, A. *Isr. J. Chem.* **1970**, *8*, 259.

(43) Marcus, R. A.; Siders, P. *J. Phys. Chem.* **1982**, *86*, 622.

(44) (a) Michel-Beyerle, M. E.; Kruger, H. W.; Haberkorn, R.; Seidlitz, H. *Chem. Phys.* **1979**, *42*, 441. (b) Nolting, F.; Staerk, H.; Weller, A. *Chem. Phys. Lett.* **1982**, *88*, 523. (c) Weller, A.; Nolting, F.; Staerk, H. *Chem. Phys. Lett.* **1983**, *96*, 24.

(45) (a) On the microsecond time scale, a small time-resolved growth in absorption is observed around 450 nm for pulsed laser excitation of argon-purged solutions of DCA or TCA in the presence of most of the donors. The triplet states of both anthracenes should be formed upon diffusive recombination of the radical cations and anions. Absorptions in this region have previously been assigned to the triplet state of DCA.[45b] No spectroscopic evidence has been obtained for triplet formation within any of the geminate ion pairs. (b) Darmanyan, A. P. *Chem. Phys. Lett.* **1984**, *110*, 89.

complex formation are recognized, and the concentration dependence of the ion yields, which occurs as a consequence of these processes, is taken into account.

E. Implications of the Inverted Region for High Quantum Yield Reactions. The present results have important consequences for the design of high quantum yield photoinduced bimolecular electron-transfer reactions. The quantum yields of product formation in such reactions are usually ca. 0.05–0.2, which means that ca. 80–95% of the incident photons that are absorbed are wasted,[1a] due to the energy-wasting return electron transfer reaction k_{-et}.[1a,3-5] The results of the present work demonstrate that the major factor influencing this rate, and hence the free-ion quantum yield, is the return electron transfer exothermicity. It is clear that those systems in which the initial electron transfer to form the ion pair is least exothermic, i.e., those reactions that store the most energy in the ion pair, undergo the slowest return electron transfer and thus have the highest quantum yields for formation of free ions. It is of course fortuitous that the ion pairs that store the most chemical energy are least likely to undergo the energy-wasting return electron transfer process. This effect accounts to a large extent for the success of cosensitization in bimolecular electron-transfer reactions,[1a,4,46] and indeed, we note that the radical-ion pair formed upon quenching of singlet DCA by biphenyl, a well-known cosensitizer system,[1a,4,46] has the highest quantum yield for free-ion formation of all of those measured.

The concept of cosensitization in electron-transfer photochemistry is schematically illustrated in Scheme II. As discussed above, the formation of a low oxidation potential donor radical cation through the direct path, i.e., via reaction of D with the excited acceptor and the subsequent intermediate, $A^{\bullet-}/D^{\bullet+}$ (path a,b, Scheme II), would generate free ions with low quantum yield (Φ_D) due to the fast return electron transfer in the geminate pair. In the cosensitized reaction, a nonreactive molecule with a high oxidation potential, the cosensitizer C, is used as the primary donor. As a consequence of the inverted region effect, return electron transfer in the pair $A^{\bullet-}/C^{\bullet+}$ is a slow reaction, which results in a high quantum yield for free radical ion formation (Φ_C). In the presence of low concentrations of D, secondary electron transfer from D to $C^{\bullet+}$ leads to $D^{\bullet+}$ with a quantum yield (Φ_C, path c–e, Scheme II) that is much higher than that of the direct path (Φ_D). This concept has been successfully applied to many electron-transfer reactions to achieve high quantum yields even in cases where the direct path did not lead to measurable product formation.[1a,4,46] The use of cosensitization is not limited to preparative photochemical applications. We have used this technique to measure quantitative transient absorption spectra of the radical cations of many donors. With this method, the donor radical cations formed via secondary electron transfer to $C^{\bullet+}$ are produced in a known, high quantum yield (Φ_C). Furthermore, relatively low concentrations of the donor are required, which is important if "self-quenching" reactions of the radical cation are possible, by either the neutral donor, or by unavoidable impurities in the donor. In this way the radical cations of *trans*- and *cis*-stilbene were easily characterized.[47]

V. Conclusions

In the present work, the factors that control the return electron transfer rate, and the important role of the inverted region in electron-transfer processes in homogeneous solution, are defined. It is demonstrated that the rates of these first-order bimolecular electron-transfer reactions can be successfully analyzed by current semiquantum mechanical theories. The factors that control the rates of such reactions have been explored, and it is determined that for the systems studied, the reactions rates are most influenced by the reaction free energy, and that the rates of the most exothermic reactions are controlled by the Marcus inverted region effect. In general, for an efficient photoinduced electron-transfer chemical reaction, the exothermicity (driving force) of the initial charge-separation process should be as small as is consistent with efficient formation of the initial charge-separated state, so that the exothermic rate restrictions that characterize electron-transfer reactions in the inverted region minimize the rate of the energy-wasting return electron transfer.

VI. Experimental Section

Materials. Acetonitrile (Baker, HPLC grade) was used as received. 9,10-Dicyanoanthracene (DCA) (Kodak) was purified by crystallization from pyridine and acetonitrile. 2,6,9,10-Tetracyanoanthracene (TCA) was prepared as described earlier[48] and was purified by chromatography on silica gel eluting with methylene chloride. *m*-Xylene (**1**; Kodak), *o*-xylene (**2**; Kodak), mesitylene (**3**; Aldrich), and 1,2,4-trimethylbenzene (**5**; Kodak) were purified by distillation. Durene (**9**; Aldrich) pentamethylbenzene (**12**; Aldrich), hexamethylbenzene (**13**; Aldrich), biphenyl (**14**; Kodak), fluorene (**17**; Kodak), 4,4′-dimethylbiphenyl (**19**; Aldrich), 2,6-dimethylnaphthalene (**20**; Aldrich), phenanthrene (**21**; Kodak), and benzophenone (Kodak) were purified by repeated crystallization from ethanol. 3,6-Dimethylphenanthrene (**23**; Aldrich) and 4,4′-dimethoxystilbene (Aldrich) were recrystallized from acetonitrile. *p*-Xylene (**4**; Aldrich Gold Label), 1,2,3,4-tetramethylbenzene (**6**; API standard reference materials), 1,2,3,5-tetramethylbenzene (**7**; API standard reference materials), 5,8-dimethyltetrahydronaphthalene (**8**; API standard reference materials), octahydrophenanthrene (**10**; API standard reference materials), octahydroanthracene (**11**; API standard reference materials), 3,3′-dimethylbiphenyl (**15**; Aldrich), naphthalene (**16**; Aldrich Gold Label), 2-methylnaphthalene (**18**; Aldrich), and 2-methylphenanthrene (**22**, Aldrich) were used as received. Samples of tritolylamine and trianisylamine were generously provided by Dr. Geoffrey Rule (Eastman Kodak).

Steady-State Spectroscopy. Steady-state emission spectra were recorded with a Spex Fluorolog 212 spectrometer. Absorption spectra were recorded by using a Perkin-Elmer Lambda-9 spectrometer, equipped with a 7000 series datastation. Solutions were analyzed in 1-cm^2 quartz cuvettes equipped with arms for freeze–pump–thaw degassing, or for argon purging. In all the experiments, oxygen was removed by one of these two methods.

Time-Resolved Spectroscopy. A conventional transient absorption apparatus was used, consisting of a Questek 2000 excimer laser (308 nm, ca. 15 ns, ca. 100 mJ) that pumped a Lumonics EPD-330 dye laser. DPS (410 nm, ca. 1 mJ), bis(MSB) (422 nm, ca. 1 mJ), and BPBD (367 nm, ca. 2 mJ) were used to excite the acceptors and other compounds. A pulsed (PRA M-305) Osram XBO-150W1 xenon arc lamp (Oriel 66060 housing, PRA 302 power supply) was used as the monitoring light source. The monitoring light was passed through an ISA H-20 monochromator and was detected by using six dynodes of an RCA 4840 photomultiplier tube (PMT). The output from the PMT was monitored with a Nicolet 4094A digital oscilloscope. Data analysis was performed on an IBM-AT computer.

Fluorescence lifetime measurements were performed by the technique of single-photon counting, using an apparatus that will be described in detail elsewhere (ref 19).

Molecular Orbital Calculations. Calculations were performed using the MOPAC package[49a] with the AM1 parameter set.[49b] Calculations on the neutral (closed-shell) species were performed using the RHF method. Calculations on the radical ions were performed using a modified UHF method, adapted from ref 49c for use with MOPAC V3.0 by J. McKelvey (Eastman Kodak), to avoid problems associated with spin contamination.

Electrochemical Measurements. Electrochemical measurements were made using the technique of square-wave voltammetry.[50a] Generally a 1 mM solution of the aromatic compound was prepared in 45:5:1 by volume methylene chloride (Fisher, HPLC grade), trifluoroacetic acid (Kodak), and trifluoroanhydride (Kodak). Activated alumina (Woelm) was added to absorb traces of moisture when necessary. The measurements were made in vials sealed with a septum. Solution preparation was carried out in a glovebag under a dry nitrogen atmosphere. For

(46) (a) Schaap, A. P.; Siddiqui, S.; Prasad, G.; Palomino, E.; Lopez, L. *J. Photochem.* **1984**, *25*, 167. (b) Arnold, D. R.; Snow, M. S. *Can. J. Chem.* **1988**, *66*, 3012. (c) Majima, T.; Pac, C.; Nakasone, A.; Sakurai, H. *J. Am. Chem. Soc.* **1981**, *103*, 4499. (d) An additional mechanism for cosensitization relies on the longer lifetime of $C^{\bullet+}$ compared to $^1A^*$, in which case donors with oxidation potentials higher than that of C can be oxidized.[1a]

(47) Lewis, F. D.; Dykstra, R. E.; Gould, I. R.; Farid, S. *J. Phys. Chem.* **1988**, *92*, 7042.

(48) Mattes, S. L.; Farid, S. *J. Am. Chem. Soc.* **1982**, *104*, 1454.

(49) (a) Stewart, J. J. P. Frank J. Seiler Research Laboratory, United States Air Force Academy, Colorado Springs, CO. (b) Dewar, M. J. S.; Zoebisch, E. G.; Healy, E. F.; Stewart, J. J. P. *J. Am. Chem. Soc.* **1985**, *107*, 3902. (c) McWeeny, R.; Diercksen, G. *J. Chem. Phys.* **1968**, *49*, 4852.

(50) (a) Osteryoung, J.; O'Dea, J. J. In *Electroanalytical Chemistry*; Bard, A. J., Ed.; Marcel Dekker: 1986; Vol. 14, p 209. (b) Mann, C. K.; Barnes, K. K. *Electrochemical Reactions in Nonaqueous Systems*; Marcel Dekker: New York, 1970; p 278.

square-voltammetry measurements a Princeton Applied Research (PAR) Model 273 potentiostat galvonastat was used interfaced to a Hewlett-Packard 9816 computer. Square-wave voltammetry measurements were made at a frequency of 5 kHz with a step height of 5 mV, and square-wave amplitude of 50 mV. A commercially available Pt electrode (Bioanalytical Systems), 10 μm in diameter, was used as a working electrode. A Pt wire or gauze constituted the counter electrode. The oxidation potentials (E^{ox}_D) given in the Tables II-IV correspond to the peak potentials obtained from the square-wave voltammetry experiments. These peak potentials are equivalent to $E^{\circ\prime}$ for reversible redox couples. The reference redox couple ferrocene/ferrocenium established the reference potential. The potentials were normalized to the SCE electrode by the addition of 0.44 V. The oxidation potential of the 4,4'-dimethoxystilbene (DMS) monitor obtained in acetonitrile by this method is 1.07 V vs SCE. The oxidation potentials of the tritolylamine (TTA) and trianisylamine (TAA) monitors are 0.75 and 0.52 V vs SCE, respectively.[50b]

Acknowledgment. We thank R. E. Moody and B. Armitage for technical assistance, J. E. Eilers for help with the MO calculations, J. R. Lenhard for the spectroelectrochemical measurement and the reduction potentials of DCA and TCA, V. D. Parker (Trondheim, Norway) for measuring the oxidation potential of biphenyl, and F. D. Saeva and R. H. Young for helpful discussions.

Registry No. 1, 108-38-3; **2**, 95-47-6; **3**, 108-67-8; **4**, 106-42-3; **5**, 95-63-6; **6**, 488-23-3; **7**, 527-53-7; **8**, 14108-88-4; **9**, 95-93-2; **10**, 29966-04-9; **11**, 1079-71-6; **12**, 700-12-9; **13**, 87-85-4; **14**, 92-52-4; **15**, 612-75-9; **16**, 91-20-3; **17**, 86-73-7; **18**, 91-57-6; **19**, 613-33-2; **20**, 581-42-0; **21**, 85-01-8; **22**, 2531-84-2; **23**, 1576-67-6; DCA, 1217-45-4; TCA, 80721-78-4; DMS, 4705-34-4; TTA, 1159-53-1; TAA, 13050-56-1; $DCA^{\bullet-}$, 22027-33-4; $Ph_2^{\bullet+}$, 34507-30-7; p-$MeOC_6H_4CH{=}CHC_6H_4$-p-$OMe^{\bullet+}$, 63464-03-9; $(p\text{-}MeC_6H_4)_3N^{\bullet+}$, 34516-45-5; $(p\text{-}MeOC_6H_4)_3N^{\bullet+}$, 34516-46-6; p-$MeC_6H_4Me^{\bullet+}$, 34510-22-0; durene radical cation, 34473-49-9; naphthalene radical cation, 34512-27-1; phenanthrene radical cation, 34504-68-2.

Coadsorption of Ferrocene-Terminated and Unsubstituted Alkanethiols on Gold: Electroactive Self-Assembled Monolayers

Christopher E. D. Chidsey,* Carolyn R. Bertozzi, T. M. Putvinski, and A. M. Mujsce

Contribution from the AT&T Bell Laboratories, Murray Hill, New Jersey 07974.
Received December 4, 1989

Abstract: Self-assembled monolayers provide an ideal system for disentangling the fundamental events in interfacial electron transfer. Coadsorption of ferrocene-terminated alkanethiols with unsubstituted n-alkanethiols on evaporated gold films yields stable, electroactive self-assembled monolayers. Monolayers containing low concentrations of alkanethiols linked to ferrocene by a polar ester group ($FcCO_2(CH_2)_nSH$, Fc = $(\eta^5\text{-}C_5H_5)Fe(\eta^5\text{-}C_5H_4)$) show thermodynamically ideal surface electrochemistry in 1 M $HClO_4$, indicating the ferrocene groups to be homogeneous and noninteracting. Higher surface concentrations or use of alkanethiols linked directly to the nonpolar ferrocene group ($Fc(CH_2)_nSH$) lead to broadened electrochemical features, indicating interactions among ferrocene groups or inhomogeneous sites. Longer chain lengths and lower ferrocene surface concentrations result in slower electron-transfer kinetics with the ferrocene groups. A fraction of the thiols in a monolayer exchange with thiols in an ethanol solution, but much of the monolayer remains unequilibrated after 10 days. Concurrent with exchange of a fraction of the electroactive adsorbates for electroinactive ones, there is a substantial decrease in the rate of electron transfer with the remaining electroactive groups. We suggest lattice and domain-boundary models of the mixed monolayers, which qualitatively explain our results and which indicate that quantitative studies of electron-transfer kinetics in this system will be very fruitful.

Detailed understanding and rational control of electron-transfer events at the electrochemical interface require structural insight and structural control. The electronic coupling between an electrode and an electroactive molecular site remains poorly understood despite extensive studies of outer-sphere electrochemical kinetics[1-3] and of chemical modification of electrode surfaces.[4-13] In the most significant work to date on the relationship between interfacial structure and electronic coupling, Li and Weaver showed that the rate of the irreversible reduction of cobalt(III) to cobalt(II) decreased exponentially with the number of atoms in the bifunctional ligand linking the cobalt(III) center to a gold surface.[14] However, the structure of that interface was unknown beyond the bond connectivities. Here we report a chemistry for incorporating a reversible, outer-sphere redox couple into an

(1) (a) Phelps, D. K.; Kornyshev, A. A.; Weaver, M. J. *J. Phys. Chem.* **1990**, *94*, 1454-1463, and references therein. (b) McManis, G. E.; Golovin, M. N.; Weaver, M. J. *J. Phys. Chem.* **1986**, *90*, 6563-6570.
(2) Yoshimori, A.; Kakitani, T.; Mataga, N. *J. Phys. Chem.* **1989**, *93*, 3694-3702.
(3) Iwasita, T.; Schmickler, W.; Schultze, J. W. *Ber. Bunsenges. Phys. Chem.* **1985**, *89*, 138-142.
(4) Murray, R. W. In *Electroanalytical Chemical Vol. 13*; Bard, A. J., Ed.; Marcel Dekker: New York, 1984; pp 191-368 and references therein.
(5) Bunding Lee, K. A.; Mowry, R.; McLennan, G.; Finklea, H. O. *J. Electroanal. Chem.* **1988**, *246*, 217-224.
(6) Bravo, B. G.; Michelhaugh, S. L.; Soriaga, M. P. *J. Electroanal. Chem.* **1988**, *241*, 199-210.
(7) Diaz, A.; Kaifer, A. E. *J. Electroanal. Chem.* **1988**, *249*, 333-338.
(8) Hickman, J. J.; Zou, C.; Ofer, D.; Harvey, P. D.; Wrighton, M. S.; Laibinis, P. E.; Bain, C. D.; Whitesides, G. M. *J. Am. Chem. Soc.* **1989**, *111*, 7271-7272.
(9) Widrig, C. A.; Majda, M. *Langmuir* **1989**, *5*, 689-695.
(10) Zhang, X.; Bard, A. J. *J. Am. Chem. Soc.* **1989**, *111*, 8098-8105.
(11) Donohue, J. J.; Buttry, D. A. *Langmuir* **1989**, *5*, 671-678.
(12) Katz, E. Y.; Solov'ev, A. A. *J. Electroanal. Chem.* **1989**, *261*, 217-222.
(13) Ueyama, S.; Isoda, S.; Maeda, M. *J. Electroanal. Chem.* **1989**, *264*, 149-156.
(14) Li, T. T.-T.; Weaver, M. J. *J. Am. Chem. Soc.* **1984**, *106*, 6107-6108.

0002-7863/90/1512-4301$02.50/0